ADVANCED ELECTRONIC MATERIALS
Open Access
www.advelectronicmat.de

Manipulation of Magnetization Switching by Ultrafast Spin-Polarized Hot-Electron Transport in Synthetic Antiferromagnet

Meiyang Ma, Zhuoyi Li, Xuezhong Ruan, Jing Wu, Ruifeng Wang, Tianyu Liu, Jun Du, Xianyang Lu,* and Yongbing Xu**

Uncovering the physical mechanisms that govern ultrafast charge and spin dynamics is becoming indispensable both at the fundamental level and to develop future spin-based electronics. Recently it has been shown that femtosecond pulsed-laser excitation of magnetic thin films produces intense and ultrafast spin-polarized hot electrons, thus attracting a lot of attention. While spin-polarized hot electrons are known to play a pivotal role in the ultrafast laser-induced demagnetization, their effect on magnetization switching remains an open issue. This study uncovers the effect of spin-polarized hot electrons generated by laser excitation on magnetization switching in a Co/Pt based perpendicular magnetic anisotropy-based synthetic antiferromagnet (p-SAF) using the time-resolved magneto-optical Kerr effect. It has been found that, at low pump fluence, the equivalent magnetic field generated by the hot-electron spin current plays a dominant role in assisting the magnetization switching of the lower layer in the antiferromagnetic configuration, while the strong thermal stability of the Ruderman Kittel Kasuya Yosida exchange interaction inhibits the further weakening of the switching field at high pump fluence. This study provides a viable way to control the magnetization switching of the antiferromagnetically exchange-coupled systems for spintronic applications with ultrafast control of the information operation.

1. Introduction

Since the discovery in 1996 by Beaurepaire et al. that a femtosecond laser pulse can quench the magnetization in nickel thin films within less than a picosecond,[1] the field of femtomagnetism has attracted thriving interest due to the potential advantages of ultrafast spin manipulation for current and future information technologies, such as data storage and spintronics.[2–4] Femtosecond pulsed lasers offer a fascinating possibility to probe a magnetic system on a time scale corresponding to the (equilibrium) exchange interaction, which is two or three orders of magnitude faster than magnetic precession. Ultrafast demagnetization, as one of the most key issues, has been the subject of intense research for more than 20 years. Initially, ultrafast demagnetization was explained by a phenomenological three-temperature model, which describes the transfer of heat between electrons, phonons, and spin baths.[1,5] Subsequently, different models based on the conservation of angular momentum have been proposed, either relying on the spin-flip scattering mediated by particles or quasiparticles,[6–16] or on the direct coupling between the photon field and the spin bath,[17,18] or considering the thermal demagnetization mechanism.[19,20] In the last decade, a new model based on superdiffusive spin transport has been mentioned, which couples the fields of ultrafast spin dynamics and stationary

M. Ma, Z. Li, X. Ruan, R. Wang, X. Lu, Y. Xu
Jiangsu Provincial Key Laboratory of Advanced Photonic and Electronic Materials
School of Electronic Science and Engineering
Nanjing University
Nanjing 210093, P. R. China
E-mail: xylu@nju.edu.cn; ybxu@nju.edu.cn

The ORCID identification number(s) for the author(s) of this article can be found under https://doi.org/10.1002/aelm.202201331.

DOI: 10.1002/aelm.202201331

J. Wu, Y. Xu
York-Nanjing Joint Center (YNJC) for Spintronics
Department of Electronic and Physics
The University of York
York YO10 5DD, UK
E-mail: jing.wu@york.ac.uk

T. Liu, J. Du
Department of Physics
Nanjing University
Nanjing 210093, P. R. China

spin transport.[21–24] It has been demonstrated that laser excited spin-polarized hot electrons can transport angular momentum to neighboring ferromagnetic (FM) layers, thus changing the orientation and magnitude of magnetization as well as leading to faster and larger demagnetization of the two antiparallel FM layers.[25–32] In more general cases, ferromagnets can even be demagnetized using only unpolarized hot electrons.[33–35]

The discovery of synthetic antiferromagnetic (SAF) materials is well suited to explore the possible magnetization switching and their mechanisms by the laser excited spin-polarized hot electrons in an antiferromagnetic coupled system.[36,37] The SAF structure typically consists of two ferromagnetic layers separated by a nonmagnetic (NM) spacer layer. According to Ruderman Kittel Kasuya Yosida (RKKY) theory,[38–40] the magnetization oscillation between the FM and antiferromagnetic (AF) alignment depends on the spin-dependent reflectivity of the conductive electrons at the FM/NM interface. The stray field can be effectively compensated by a SAF structure to improve the storage stability of the device. At the same time, since the net magnetic moment of the SAF structure is small or even zero, it is introduced into the spin valve as the free layer or the pinned layer, which can reduce the coupling between layers and reduce the influence of the demagnetizing field of the pinned layer on the free layer.[41] Different from a single ferromagnetic layer, a SAF structure can switch the magnetization between parallel and antiparallel under the regulation of the external magnetic field. This unique structure serves as a promising approach for the designing of spin current-controlled spintronic devices.[42,43] Ju et al. studied the photoinduced modulation of an exchange-biased ferromagnetic/antiferromagnetic bilayer film (NiFe/NiO).[44,45] It is demonstrated that the coercivity extracted from the transient hysteresis loop is a stable parameter in describing the ultrafast photoinduced spin dynamics for both reversible and irreversible behaviors.[46]

To uncover the effect of spin-polarized hot-electrons generated by laser excitation on magnetization switching in SAF, in this work, we have carried out a systematic study of a $[Pt/Co]_4/Ru/[Co/Pt]_4$ based SAF structure by using the time-resolved magneto-optical Kerr effect (TRMOKE). The optically induced changes in the magnetization of the sample were recorded by measuring the transient changes in the polar Kerr rotation. We have experimentally observed that the evidence of spin-polarized hot electrons will assist the magnetization switching of the lower ferromagnetic layer at low pump fluences. This phenomenon strongly depends on the relative orientation of magnetization between the layers. The different trends in the timeline of the magnetization state near the switching field and on the antiferromagnetic platform are found to reflect its irreversible and reversible processes, respectively. Based on our experiments, the role of spin-polarized hot electrons is analyzed in detail, providing a clear physical picture of the underlying fundamental mechanism.

2. Results and Discussion

The layer structure of the composite film and the concept of how we generate a net spin current in ultrafast demagnetization are shown schematically in **Figure 1**a. After excitation of the sample by a laser pulse, spin-polarized hot electrons are created in both ferromagnetic layers and are transported between the two layers. Whether there is a net spin current depends on the relative orientation of the magnetization of the two ferromagnetic layers. For parallel (P) alignments, the spin currents between the two layers cancel, resulting in a net spin current of zero. In contrast, for antiparallel (AP) alignment, a net spin current is induced. To experimentally explore the manipulation of magnetization switching by net spin-polarized hot electron current, we have properly designed the sample structure in which the identical $[Co\text{-}Pt]_4$ multilayers are antiferromagnetic coupled through a thin spacer. The use of two identical ferromagnetic layers is intended to produce the same number of spin-polarized hot electrons during laser excitation, thus simplifying interpretation of experimental results. The pure thermal effect due to laser energy deposition can be ruled out as shown in the supplementary information and we expect to be able to detect the effect of the only spin current on its magnetization switching.

Figure 1b shows the out-of-plane hysteresis loop of the sample measured by vibrating sample magnetometer (VSM). The upper and lower ferromagnetic layers are antiferromagnetically coupled and show two different switching fields separated by a large antiferromagnetic plateau. With the same thickness of the two ferromagnetic layers, there should be no net magnetization in the AP state because the magnetization in opposite directions is fully compensated. However, the steady-state MOKE signal was measured using only probe light in the TRMOKE system, and a different result was obtained, as shown in Figure 1c. The nonzero MOKE signal in the AP state is due to the different Kerr sensitivities of each ferromagnetic multilayer, where the upper Co-Pt multilayer contributes more to the total Kerr signal.[30,32] Note that the switching fields $H_{P\text{-}AP}$ and $H_{AP\text{-}P}$ at ≈2.2 kOe and 3.0 kOe correspond to the magnetization configuration of the sample from parallel to antiparallel and from antiparallel to parallel, respectively. At the same time, they correspond to the magnetization reversal of the upper and lower ferromagnetic layer. This allows us to distinguish the magnetization switching of different ferromagnetic layers more clearly.

Figure 2a depicts the demagnetization curves under a pump fluence of 0.32 mJ cm^{-2} for the P and AP states, corresponding to the applied magnetic fields of 4.4 kOe and 0 kOe, respectively. Comparing the demagnetization curves of the P and AP states, it can be found that there is faster demagnetization in the AP state. To obtain a more quantitative understanding of the femtosecond laser-induced demagnetization dynamics, a so-called three-temperature model is used to describe it.[1,30,47] This phenomenological model depicts how the energy of the laser is redistributed among the electrons, spins and lattice after it is absorbed by the electron system. Fitting experimental data with this model enables us to extract characteristic parameters such as the time zero and demagnetization time τ_M:

$$-\frac{\Delta M_z(t-t_0)}{M_{0,z}} = \left\{\left[A_1F(\tau_0,t-t_0) - \frac{(A_2\tau_E - A_1\tau_M)e^{-\frac{t-t_0}{\tau_M}}}{\tau_E-\tau_M} - \frac{\tau_E(A_1-A_2)e^{-\frac{t-t_0}{\tau_E}}}{\tau_E-\tau_M}\right]\Theta(t-t_0) + A_3\delta(t-t_0)\right\} * \Gamma(t-t_0) \quad (1)$$

ADVANCED ELECTRONIC MATERIALS
Open Access
www.advelectronicmat.de

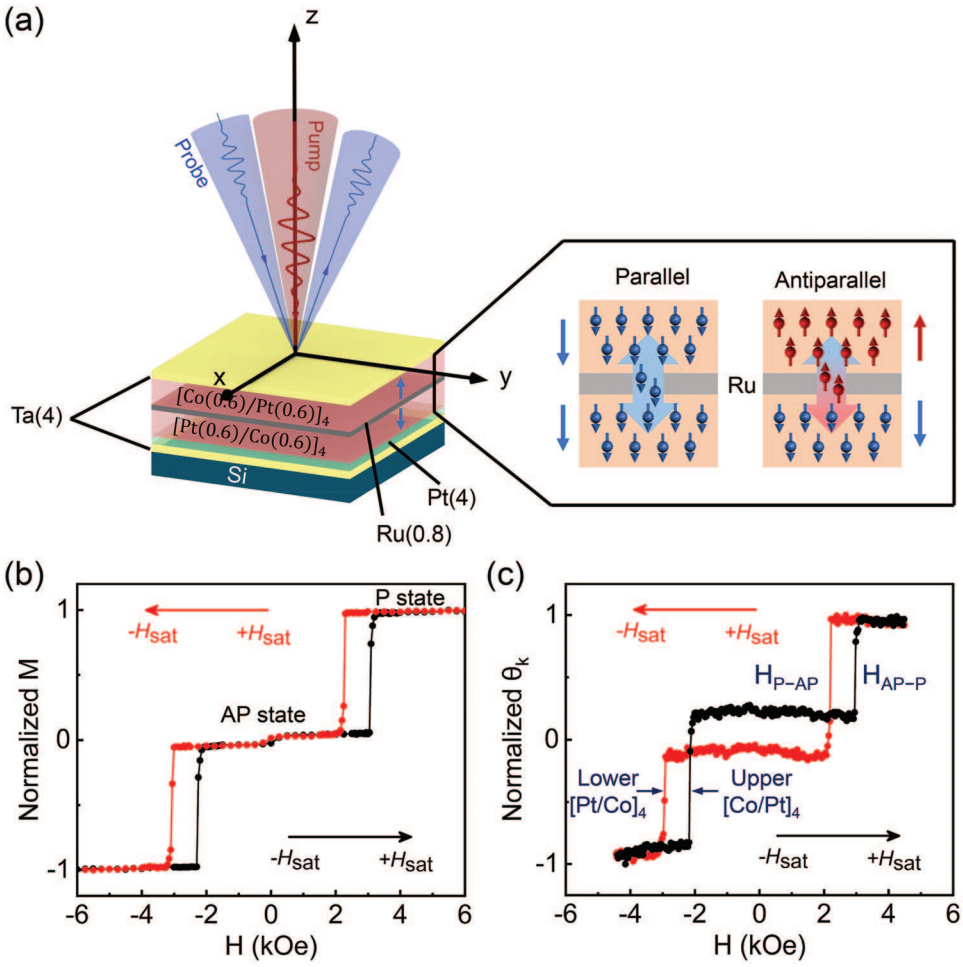

Figure 1. a) Experimental setup and SAF sample schematics. The excitation of the pulsed laser results in the generation of hot electrons in both ferromagnetic layers. The net spin current depends on the relative orientation between the magnetization of the two ferromagnetic layers. Hysteresis loops measured by b) VSM and c) MOKE. The black and red lines represent the process of the magnetic field going from negative to positive and from positive to negative, respectively.

where t_0 is the time zero, $\Gamma(t - t_0)$ is the Gaussian laser pulse, $*$ represents the convolution product, $\Theta(t - t_0)$ is the step function, and $\delta(t - t_0)$ is the Dirac delta function. The constant A_1 represents the amplitude of demagnetization obtained after equilibrium between electrons, spins, and lattice is restored, while A_2 is proportional to the initial electron temperature rise. The constant A_3 represents the magnitude of the state filling effects during pump-probe temporal overlap, which can be well described by a delta function. The function $F(\tau_0, t - t_0)$ describes the process of heat diffusion cooling in terms of the inverse square root, where $\tau_0 \gg \tau_E, \tau_M$. The two critical parameters τ_M and τ_E are the ultrafast demagnetization time and the electron–phonon relaxation time, respectively. The fitted solid curves are also plotted in Figure 2a. The demagnetization curves of the P state and AP state under different pump fluences were also measured, and the corresponding demagnetization time was extracted, as shown in Figure S1, Supporting Information. The demagnetization time does not change significantly with increasing pump fluence and remains at ≈76 and 35 ps in the P state and AP state, respectively. Hence, the demagnetization process in the AP state is 54% faster than that in the P state.

With the so-called three-temperature model, not only the demagnetization time can be obtained, but also the position of time zero can be determined. After that, we study the change in magnetization switching at different delay times under different pump fluences. Figure 2b displays "snapshots" of the transient hysteresis loops measured with a pump fluence of 0.32 mJ cm^{-2} at probe delays of t = –0.001, 0.299, 1.332, 7.599, and 140.932 ps. The amplitude of the transient hysteresis loops corresponds to that of the demagnetization curve at different delay times. At such a weak pump fluence, the switching of the two ferromagnetic layers is not affected, consistent with the steady-state hysteresis loop. Furthermore, the switching magnetic field does not change on the time scale. With the pump fluence up to 0.96 mJ cm^{-2}, the transient hysteresis loop changes (Figure 2c): The switch of one ferromagnetic layer is hardly affected, while the switch of the other layer is "softened," and the corresponding coercivity decreases from 3.0 to 2.5 kOe. This softening of magnetization switching seems to be common in pulsed laser measurements, generally because of the change in magnetic anisotropy caused by laser energy deposition on the sample surface.[48–51] Counterintuitively, it is the

ADVANCED ELECTRONIC MATERIALS
Open Access
www.advelectronicmat.de

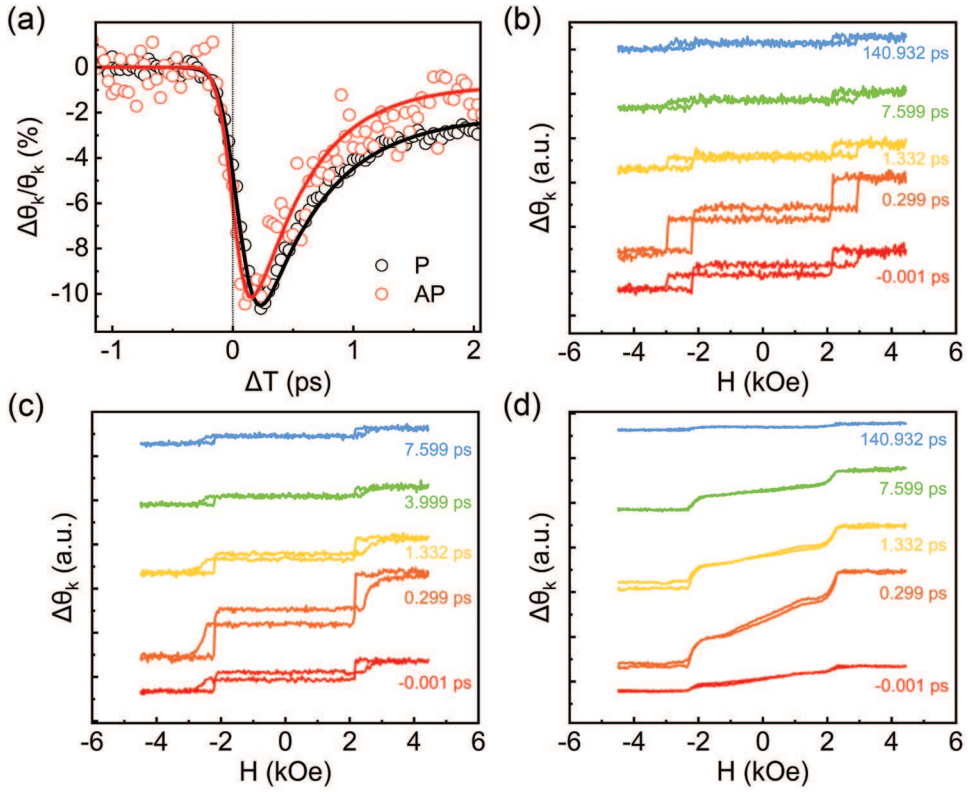

Figure 2. a) TRMOKE measured in the parallel and antiparallel states with a pump fluence of 0.32 mJ cm^{-2}. The solid lines are fits to the experimental data. Time-delayed transient hysteresis loops measured at pump fluences of b) 0.32 mJ cm^{-2}, c) 0.96 mJ cm^{-2}, and d) 4.00 mJ cm^{-2}.

lower rather than the upper ferromagnetic layer that is affected first. It is believed that the spin-polarized transport of hot electrons introduced by an ultrafast laser causes a change in magnetic anisotropy and coercivity in the lower ferromagnetic layer, which will be explained in the following. As the pump fluence further increases, the transient hysteresis loops with different delay times measured at a pump fluence of 4.00 mJ cm^{-2} in Figure 2d are significantly different from the previous data. In addition to the observed further reduction in the coercivity of the lower ferromagnetic layer, the slope of the antiferromagnetic plateau increases first and then decreases on the time scale.

First, we focus on the change in the time scale of the parameters extracted from the time-delayed transient hysteresis loops. There is no change in the magnitude of the switching magnetic field extracted from the time-delayed transient hysteresis loops under a pump fluence of 4.00 mJ cm^{-2} as a function of delay time, as shown in **Figure 3**a. This is because averaging over N pulse pairs washes out the coercivity characteristics in time, whereas a maximum reduction in coercivity can always be detected depending on the pump fluence.[48,51] However, the slope of the antiferromagnetic platform near zero magnetic field of the time-delayed transient hysteresis loops changes significantly on the time scale at a high pump fluence of 4.00 mJ cm^{-2}. The slope of the normalized curve is extracted and shown in Figure 3b along with the demagnetization curve in the P state at the same pump fluence. The maximum demagnetization occurs at ≈0.5 ps and then presents a slower recovery process. The change in the extracted slope on the time axis shows a different trend from the demagnetization curve. It reached its maximum at 0.132 ps, followed by a rapid recovery process, and fully recovered to ≈0 at 140 ps. This phenomenon is not contrary to previous reports that the switching field does not change on the timeline because the antiferromagnetic plateau region always returns to the original state before the next pulse of pump laser arrives. The difference between the demagnetization curve and the extraction slope on the time axis is due to the distinct relaxation process. The former reflects the change in spin temperature, and the latter reflects the change in the anisotropy of the magnetic moment. When the pump light hits the sample, the electrons absorb energy and become hot electrons. The thermalization of the electrons affects the anisotropy of the carrying magnetic moment, which is reflected in the uniform rotation of the magnetic moment away from the interface. The fast and slow recovery processes correspond to the electron-spin coupling and the overall thermal effect, respectively.

In order to vividly reveal the different trends of the magnitude of the switching magnetic field and the slope of the antiferromagnetic platform on the time scale, we interpret them as schematics shown in Figure 3c and Figure 3d for the situation of the first and all subsequent pump pulses, respectively. Since we use a pulsed Ti:sapphire regenerative amplifier with a repetition rate of 1 kHz to achieve the measurement, a separate pump-probe pair hits the sample every millisecond. The time interval between the two pump pulses is long enough to consider the heat diffusion or heat accumulation effect to be over

ADVANCED ELECTRONIC MATERIALS
Open Access
www.advelectronicmat.de

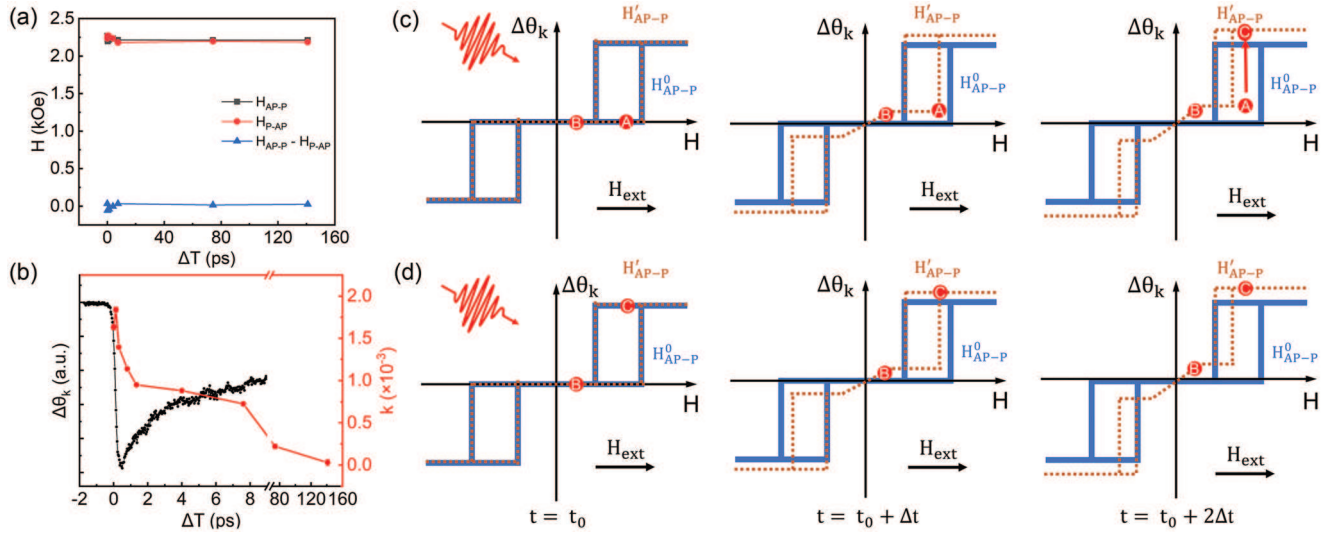

Figure 3. a) $H_{AP\text{-}P}$, $H_{P\text{-}AP}$, and $H_{AP\text{-}P} - H_{P\text{-}AP}$ extracted from time-delayed transient hysteresis loops under a pump fluence of 4.00 mJ cm^{-2} as a function of delay time. b) The demagnetization curve in the P state and the slope of the antiferromagnetic plateau extracted by the transient hysteresis loop as a function of time at a pump fluence of 4.00 mJ cm^{-2}. c) Schematic of the magnetization state change induced by the first pump pulse. d) Schematic of the magnetization state change induced by the second and all following pump pulses.

before the arrival of the next pump pulse. Figure 3c shows the effect of the first pump pulse on the magnetization state of the transient hysteresis loop. Suppose that the magnetization states A and B are located near the coercivity of the lower ferromagnetic layer and the antiferromagnetic platform, respectively, and the pump fluence is large. No coercivity change was observed after the initial excitation (Figure 3c, left). However, the reduction of the coercivity of the lower ferromagnetic layer and the tilt of the antiferromagnetic platform will change the magnetization states of A and B after the time interval Δt. After a sufficiently long time interval of $2\Delta t$, the reduction of coercivity is sufficient to allow switching from magnetization state A to C on the transient hysteresis loop. Magnetization state B is still located on the tilted antiferromagnetic platform. Both the coercivity and the antiferromagnetic platform will recover before the second pump pulse arrives (Figure 3d, left). However, this recovery is not accompanied by a reorientation of the magnetization to the initial direction, since the switching is an irreversible process in a slowly changing quasistatic magnetic field.[51] Eventually, the second and any subsequent pump pulse will encounter a new magnetization state C, and no coercivity dynamic change can be observed. An averaging procedure over N pulse pairs will wash out the coercivity characteristics in time, whereas a maximum reduction in coercivity can always be detected depending on the pump fluence. Unlike magnetized state A, magnetized state B located on an antiferromagnetic platform always returns to the same position so that the corresponding slope change caused by the heat effect can be observed on the timeline.

In the following, the effect of the increasing pump fluence on the magnetization switching is discussed. The magnetization configuration corresponding to the transient hysteresis loop at different pump fluences is shown in Figure S4, Supporting Information. The behavior of the pump fluence on magnetization switching, obtained by plotting $H_{AP\text{-}P}$, $H_{P\text{-}AP}$, and $H_{AP\text{-}P} - H_{P\text{-}AP}$ as a function of pump fluence, is depicted in **Figure 4**a. In the red region, $H_{AP\text{-}P}$ decreases with the increase of pump fluence until it is consistent with $H_{P\text{-}AP}$, which shows almost no change. Considering the significant effect of spin-polarized hot electrons to the magnetization switch of SAF sample, we propose a model to explain the observed different switching of magnetization in the upper and lower ferromagnetic layers after laser excitation, as shown by the schematic diagram in Figure 4. Figure 4b shows the initial response of the sample to laser excitation in the AP state. The laser pulse excites conduction electrons throughout the whole stack, leading to a top-to-bottom spin current I_{down} and a bottom-to-top spin current I_{up}. When these spin-polarized hot electrons reach the adjacent magnetic layer, as shown in Figure 4c, their transverse angular momentum is absorbed almost instantaneously by the local magnetization.[52,53] The net spin current $I_{net} = I_{down} + I_{up}$ exerts an equivalent magnetic field H_{eff} on the magnetic layer and assists in the reversal of the magnetization of the lower layer driven by an applied magnetic field H_{appl}, leading to the decrease of $H_{AP\text{-}P}$. That is, the decrease in $H_{AP\text{-}P}$ is equal to the magnitude of the equivalent magnetic field H_{eff} generated by the hot-electron spin current. The increase in pump fluence will enhance the transmission of spin-polarized hot electrons between the two layers, resulting in a larger equivalent magnetic field, so that the reversing magnetic field corresponding to the magnetization of lower layer continues to decrease. While the magnetization of the upper layer cannot be changed due to the fixed direction of the external magnetic field. Conversely in the P state, the net spin current $I_{net} = I_{down} + I_{up}$ is zero for the assumption of local charge neutrality (Figure 4d). Without the effective magnetic field generated by the net spin current, the magnetization of the upper layer switches to the opposite orientation under the action of RKKY exchange interaction as the external magnetic field decreases (Figure 4e). However, when $H_{AP\text{-}P}$ is reduced

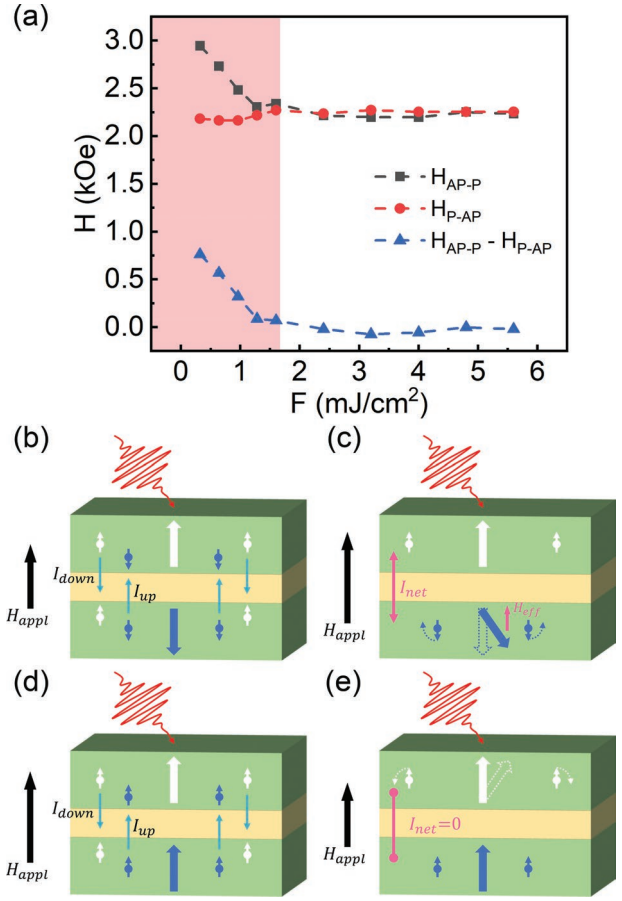

Figure 4. a) $H_{AP\text{-}P}$, $H_{P\text{-}AP}$, and $H_{AP\text{-}P} - H_{P\text{-}AP}$ as a function of pump fluence. Schematic diagrams of spin-momentum transfer in b) AP and d) P states after laser excitation. c) Change of the orientation of the magnetization due to net spin current of excited electrons and the applied magnetic field (from AP to P). e) Change of the orientation of the magnetization due to the applied magnetic field (from P to AP).

to the same size as $H_{P\text{-}AP}$, the RKKY exchange interaction still exists, which inhibits the further assisted switching of the magnetization of the lower layer by the spin-polarized hot electrons in the AP state. It is noted that to quantitatively distinguish I_{down} and I_{up} contributions certainly worth further investigation.

3. Conclusion

In summary, by probing the transient hysteresis loops of synthetic antiferromagnetic structures on ultrafast time scales, we are able to elucidate the effect of spin-polarized hot electrons on the switching of the magnetization, as well as the influence of heat effects on the magnetization of the sample on time scales. Spin-polarized hot-electron transport leads to asymmetric changes in the switching of the upper and lower ferromagnetic layers at low pump fluence, which results from the net spin current only when the magnetization directions of the two are in antiparallel. It is because of the strong thermal stability of RKKY exchange interaction that the further assisted reversal of the magnetization of the lower layer in AP state by spin-polarized hot electrons is inhibited. Our discovery provides fundamental insight into the effect of spin-polarized hot electrons on magnetization switching and is relevant for identifying the role of the interface in ultrafast spin dynamics. We demonstrated that it is possible to regulate the magnetization of the individual ferromagnetic layer in an antiferromagnetically coupled system in a controlled way by injecting photoexcited spin-polarized hot electrons.

4. Experimental Section

Sample Preparation and Vibrating Sample Magnetometer Measurement: Samples were grown by high-vacuum magnetron sputtering onto Si substrates with a native oxide at a base pressure of less than 1×10^7 Pa. The stack of SAF consists of Ta (4)/Pt (4)/[Pt (0.6)/Co (0.6)]$_4$/Ru (0.8)/[Co (0.6)/Pt (0.6)]$_4$/Ta (4) (thicknesses in nanometers). The static magnetic properties were measured by a VSM at room temperature.

Time-Resolved Magneto-Optical Kerr Effect Measurements: The magnetization dynamics were acquired by the TR-MOKE technique using a pulsed Ti:sapphire regenerative amplifier with a central wavelength of 800 nm, a pulse duration of ≈50 fs, and a repetition rate of 1 kHz. The dynamic behaviors were excited by an intense pump pulse laser (800 nm), and the transient MOKE signals were detected by a weak probe beam (400 nm) with a time delay. The pump beam normally incidents on the sample with a spot size of 400 µm in diameter, and the incident angle of the probe beam was ≈4° away from the normal direction of the film plane with a spot size of 250 µm in diameter. The magnetic field was applied normally to the sample surface. In this geometry, the Kerr rotation was sensitive only to the variation in the out-of-plane magnetization component.

Supporting Information

Supporting Information is available from the Wiley Online Library or from the author.

Acknowledgements

This work was supported by the Natural Science Foundation of Jiangsu Province of China (Grant Nos. BK20200307, BK20192006, BK20180056, and BK20211144), the National Key Research and Development Program of China (Grant No. 2021YFB3601600), and the National Natural Science Foundation of China (Grant Nos. 12104216, 61427812, 11774160, and 61805116).

Conflict of Interest

The authors declare no conflict of interest.

Data Availability Statement

The data that support the findings of this study are available from the corresponding author upon reasonable request.

Keywords

spin-polarized hot-electron transport, spintronics, synthetic antiferromagnets, ultrafast magnetization dynamics and switching

Received: December 16, 2022
Revised: January 17, 2023
Published online: March 12, 2023

[1] E. Beaurepaire, J. C. Merle, A. Daunois, J. Y. Bigot, *Phys. Rev. Lett.* **1996**, *76*, 4250.
[2] Y. Xu, M. Deb, G. Malinowski, M. Hehn, W. S. Zhao, S. Mangin, *Adv. Mater.* **2017**, *29*, 1703474.
[3] A. Stupakiewicz, K. Szerenos, D. Afanasiev, A. Kirilyuk, A. V. Kimel, *Nature* **2017**, *542*, 71.
[4] J. Walowski, M. Munzenberg, *J. Appl. Phys.* **2016**, *120*, 140901.
[5] A. Kirilyuk, A. V. Kimel, T. Rasing, *Rev. Mod. Phys.* **2010**, *82*, 2731.
[6] B. Koopmans, J. J. M. Ruigrok, F. D. Longa, W. J. M. de Jonge, *Phys. Rev. Lett.* **2005**, *95*, 267207.
[7] M. Cinchetti, M. S. Albaneda, D. Hoffmann, T. Roth, J. P. Wustenberg, M. Krauss, O. Andreyev, H. C. Schneider, M. Bauer, M. Aeschlimann, *Phys. Rev. Lett.* **2006**, *97*, 177201.
[8] C. Stamm, T. Kachel, N. Pontius, R. Mitzner, T. Quast, K. Holldack, S. Khan, C. Lupulescu, E. F. Aziz, M. Wietstruk, H. A. Durr, W. Eberhardt, *Nat. Mater.* **2007**, *6*, 740.
[9] E. Carpene, E. Mancini, C. Dallera, M. Brenna, E. Puppin, S. De Silvestri, *Phys. Rev. B* **2008**, *78*, 174422.
[10] M. Krauss, T. Roth, S. Alebrand, D. Steil, M. Cinchetti, M. Aeschlimann, H. C. Schneider, *Phys. Rev. B* **2009**, *80*, 180407.
[11] B. Koopmans, G. Malinowski, F. D. Longa, D. Steiauf, M. Faehnle, T. Roth, M. Cinchetti, M. Aeschlimann, *Nat. Mater.* **2010**, *9*, 259.
[12] A. B. Schmidt, M. Pickel, M. Donath, P. Buczek, A. Ernst, V. P. Zhukov, P. M. Echenique, L. M. Sandratskii, E. V. Chulkov, M. Weinelt, *Phys. Rev. Lett.* **2010**, *105*, 197401.
[13] K. Carva, M. Battiato, P. M. Oppeneer, *Phys. Rev. Lett.* **2011**, *107*, 207201.
[14] S. Essert, H. C. Schneider, *Phys. Rev. B* **2011**, 84, 224405.
[15] K. Carva, M. Battiato, D. Legut, P. M. Oppeneer, *Phys. Rev. B* **2013**, *87*, 184425.
[16] B. Y. Mueller, A. Baral, S. Vollmar, M. Cinchetti, M. Aeschlimann, H. C. Schneider, B. Rethfeld, *Phys. Rev. Lett.* **2013**, *111*, 167204.
[17] J. Y. Bigot, M. Vomir, E. Beaurepaire, *Nat. Phys.* **2009**, *5*, 515.
[18] H. Vonesch, J. Y. Bigot, *Phys. Rev. B* **2012**, *85*, 180407.
[19] U. Atxitia, O. Chubykalo-Fesenko, J. Walowski, A. Mann, M. Munzenberg, *Phys. Rev. B* **2010**, *81*, 174401.
[20] N. Kazantseva, U. Nowak, R. W. Chantrell, J. Hohlfeld, A. Rebei, *EPL* **2008**, *81*, 27004.
[21] M. Battiato, K. Carva, P. M. Oppeneer, *Phys. Rev. Lett.* **2010**, *105*, 027203.
[22] R. Jansen, *J. Phys. D: Appl. Phys.* **2003**, *36*, R289.
[23] M. Battiato, K. Carva, P. M. Oppeneer, *Phys. Rev. B* **2012**, *86*, 024404.
[24] A. Melnikov, I. Razdolski, T. O. Wehling, E. T. Papaioannou, V. Roddatis, P. Fumagalli, O. Aktsipetrov, A. I. Lichtenstein, U. Bovensiepen, *Phys. Rev. Lett.* **2011**, *107*, 076601.
[25] D. Rudolf, C. La-O-Vorakiat, M. Battiato, R. Adam, J. M. Shaw, E. Turgut, P. Maldonado, S. Mathias, P. Grychtol, H. T. Nembach, T. J. Silva, M. Aeschlimann, H. C. Kapteyn, M. M. Murnane, C. M. Schneider, P. M. Oppeneer, *Nat. Commun.* **2012**, *3*, 1037.
[26] G. M. Choi, B. C. Min, K. J. Lee, D. G. Cahill, *Nat. Commun.* **2014**, *5*, 4334.
[27] A. J. Schellekens, K. C. Kuiper, R. de Wit, B. Koopmans, *Nat. Commun.* **2014**, *5*, 4333.
[28] G. M. Choi, C. H. Moon, B. C. Min, K. J. Lee, D. G. Cahill, *Nat. Phys.* **2015**, *11*, 576.
[29] C. T. Wang, Y. M. Liu, *Nano Convergence* **2020**, *7*, 35.
[30] G. Malinowski, F. D. Longa, J. H. H. Rietjens, P. V. Paluskar, R. Huijink, H. J. M. Swagten, B. Koopmans, *Nat. Phys.* **2008**, *4*, 855.
[31] W. He, T. Zhu, X. Q. Zhang, H. T. Yang, Z. H. Cheng, *Sci. Rep.* **2013**, *3*, 2883.
[32] A. De, S. Arekapudi, L. Koch, F. Samad, S. N. Panda, B. Bohm, O. Hellwig, A. Barman, *ACS Appl. Mater. Interfaces* **2022**, *14*, 13970.
[33] N. Bergeard, M. Hehn, S. Mangin, G. Lengaigne, F. Montaigne, M. L. M. Lalieu, B. Koopmans, G. Malinowski, *Phys. Rev. Lett.* **2016**, *117*, 147203.
[34] A. Eschenlohr, M. Battiato, R. Maldonado, N. Pontius, T. Kachel, K. Holldack, R. Mitzner, A. Fohlisch, P. M. Oppeneer, C. Stamm, *Nat. Mater.* **2013**, *12*, 332.
[35] B. Vodungbo, B. Tudu, J. Perron, R. Delaunay, L. Muller, M. H. Berntsen, G. Grubel, G. Malinowski, C. Weier, J. Gautier, G. Lambert, P. Zeitoun, C. Gutt, E. Jal, A. H. Reid, P. W. Granitzka, N. Jaouen, G. L. Dakovski, S. Moeller, M. P. Minitti, A. Mitra, S. Carron, B. Pfau, C. V. K. Schmising, M. Schneider, S. Eisebitt, J. Luning, *Sci. Rep.* **2016**, *6*, 18970.
[36] R. A. Duine, K. J. Lee, S. S. P. Parkin, M. D. Stiles, *Nat. Phys.* **2018**, *14*, 217.
[37] X. H. Liu, K. W. Edmonds, Z. P. Zhou, K. Y. Wang, *Phys. Rev. Appl.* **2020**, *13*, 014059.
[38] P. Bruno, C. Chappert, *Phys. Rev. Lett.* **1991**, *67*, 1602.
[39] S. Mangin, D. Ravelosona, J. A. Katine, M. J. Carey, B. D. Terris, E. E. Fullerton, *Nat. Mater.* **2006**, *5*, 210.
[40] M. D. Stiles, *J. Magn. Magn. Mater.* **1999**, *200*, 322.
[41] Z. R. Tadisina, S. Gupta, P. LeClair, T. Mewes, *J. Vac. Sci. Technol., A* **2008**, *26*, 735.
[42] T. Jungwirth, X. Marti, P. Wadley, J. Wunderlich, *Nat. Nanotechnol.* **2016**, *11*, 231.
[43] R. Cheng, M. W. Daniels, J. G. Zhu, D. Xiao, *Sci. Rep.* **2016**, *6*, 24223.
[44] G. P. Ju, A. V. Nurmikko, R. F. C. Farrow, R. F. Marks, M. J. Carey, B. A. Gurney, *Phys. Rev. B* **1998**, *58*, R11857.
[45] G. P. Ju, A. V. Nurmikko, R. F. C. Farrow, R. F. Marks, M. J. Carey, B. A. Gurney, *Phys. Rev. Lett.* **1999**, *82*, 3705.
[46] J. Shim, C. Kim, H. Piao, S. Lee, K. M. Lee, J. Jeong, S. Park, Y. S. Choi, D. E. Kim, D. Kim, *Phys. Status Solidi B* **2020**, *257*, 1900307.
[47] F. D. Longa, J. T. Kohlhepp, W. J. M. de Jonge, B. Koopmans, *Phys. Rev. B* **2007**, *75*, 224431.
[48] S. Li, Z. Chen, C. Cheng, J. Li, S. Zhou, T. Lai, *Proc. SPIE 8782, 2012 International Workshop on Information Storage and Ninth International Symposium on Optical Storage, 87820Q*, **2012**, https://doi.org/10.1117/12.2016670.
[49] X. D. Liu, Z. Xu, R. X. Gao, H. N. Hu, Z. F. Chen, Z. X. Wang, J. Du, S. M. Zhou, T. S. Lai, *Appl. Phys. Lett.* **2008**, *92*, 232501.
[50] Y. Ren, H. Zhao, Z. Z. Zhang, Q. Y. Jin, *Appl. Phys. Lett.* **2008**, *92*, 162513.
[51] T. Roth, D. Steil, D. Hoffmann, M. Bauer, M. Cinchetti, M. Aeschlimann, *J. Phys. D: Appl. Phys.* **2008**, *41*, 164001.
[52] M. D. Stiles, A. Zangwill, *Phys. Rev. B* **2002**, *66*, 014407.
[53] J. W. Zhang, P. M. Levy, S. F. Zhang, V. Antropov, *Phys. Rev. Lett.* **2004**, *93*, 256602.